Functional Phenotyping of Human Plasma Using a 361-Fluorogenic Substrate Biosensing Microarray

Dhaval N. Gosalia,[1] William S. Denney,[2] Cleo M. Salisbury,[3] Jonathan A. Ellman,[3] Scott L. Diamond[1,2]

[1]Department of Bioengineering, Institute for Medicine and Engineering, University of Pennsylvania, Philadelphia, PA 19104-6281; telephone: 215-573-5702; fax: 215-573-7227; e-mail: sld@seas.upenn.edu
[2]Department of Chemical and Biomolecular Engineering, Institute for Medicine and Engineering, University of Pennsylvania, Philadelphia, PA 19104-6281
[3]Department of Chemistry, Center for New Directions in Organic Synthesis, University of California, Berkeley, CA

Received 13 December 2005; accepted 9 March 2006

Published online 30 March 2006 in Wiley InterScience (www.interscience.wiley.com). DOI: 10.1002/bit.20927

Abstract: A microarray presenting glycerol nanodroplets of fluorogenic peptide substrates was used as a biosensor for the detection of multiple enzyme activities within human plasma. Using 10 different plasma proteases (kallikrein, factor XIIa, factor XIa, factor IXa, factor VIIa, factor Xa, thrombin, activated protein C, uPA and plasmin) and a 361-compound fluorogenic substrate library (Ac-AIa-P_3-P_2-Arg-coumarin for P = all amino acids except Cys), a database was created for deconvoluting the relative activity of each individual enzyme signal in human plasma treated with various activators (calcium, kaolin, or uPA). Three separate deconvolution protocols were tested: searching for ''optimal'' sensing substrate sequences for a set of 5 enzymes and using these substrates to detect protease signals in plasma; ranking the ''optimal'' sensing substrates for 10 proteases using local error minimization, resulting in a set of substrates which were bundled via weighted averaging into a super-pixel that had biosensing properties not obtainable by any individual fluorogenic substrate; and treating each 361-element map measured for each plasma preparation as a weighted sum of the 10 maps obtained for the 10 purified enzymes using a global error minimization. The similarity of the results from these latter two protocols indicated that a small subset of $<$90 substrates contained the majority of biochemical information. The results were consistent with the state of the coagulation cascade expected when treated with the given activators. This method may allow development of future biosensors using minimal and non-specific markers. These substrates can be applied to real-time diagnostic biosensing of complex protease mixtures.

Keywords: protease; coagulation; microarray

INTRODUCTION

As a consequence of its close contact with vascularized organs, it is thought that blood biochemistry reflects the physiological or pathological state of the body (Bertina et al., 1994; Burke, 2003; Schneppenheim et al., 2001). Precisely because blood is biomarker-rich (Anderson and Anderson, 2002; Anderson et al., 2004; Fujii et al., 2005; Liotta et al., 2003) and can be routinely collected in clinical settings, rapid and thorough analysis of blood is a key goal for diagnostic and prognostic proteomics.

However, proteomic analysis of blood is complicated by the fact that human blood plasma is a complex milieu of interacting proteins with abundances spanning many orders of magnitude. For example, the concentration of endogenous tissue factor may be in the low femtomolar range (Bogdanov et al., 2003; Butenas et al., 2005; Lo and Diamond, 2004), whereas fibrinogen concentrations are often six orders of magnitude greater, in the low micromolar range. Furthermore, the proteins in blood plasma are dynamic, as exemplified by the well-known protease cascades of coagulation, complement activation, and fibrinolysis.

One of the most important protein networks in the blood is the tissue factor-initiated blood coagulation cascade (Fig. 1). The kinetics of the full reaction network are fairly well described (Hockin et al., 2002) and the importance of this cascade is well documented. Problems with the coagulation cascade such as factor V Leiden, von Willebrand's disease, and hemophilia A and B demonstrate strong genotype/phenotype linkages in blood biology (Bertina et al., 1994; Burke, 2003; Schneppenheim et al., 2001). Capturing the activation states for all of the blood coagulation cascade proteases would allow distinct activity maps to be created for the different transient states of a plasma sample. Ideally, a novel kinetic signature could be detected by comparing such activity maps of normal and diseased plasma to reveal diagnostic information.

Mass spectrometric (MS) methods in tandem with liquid chromatography and 2-dimensional gel electrophoresis (2DGE) are currently used for the detection of biomarkers in blood diagnostics (Petricoin et al., 2004). MS- and

Correspondence to: S.L. Diamond
D.N. Gosalia and S.L. Diamond contributed equally to this work.

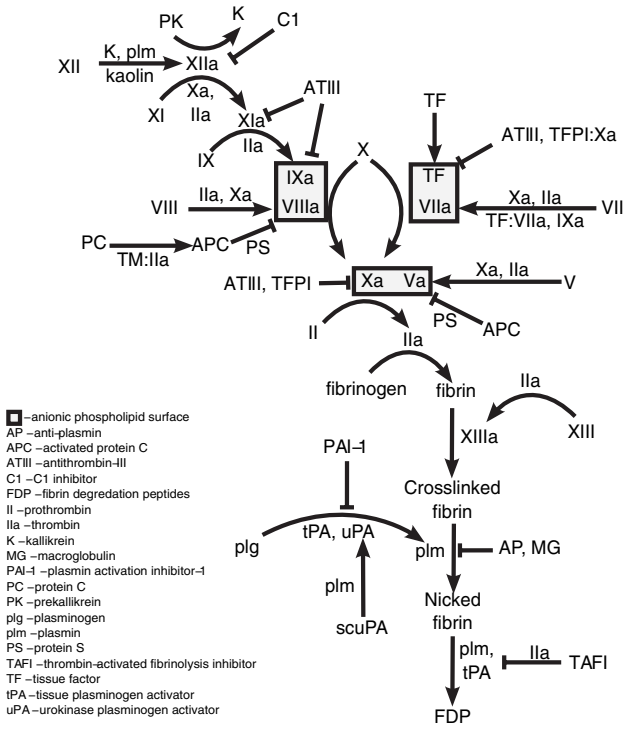

Figure 1. The coagulation pathways. This is a diagram of the contact (XII activated) and tissue factor pathways of coagulation. Note that II is prothrombin and IIa is thrombin.

gel-based proteomic methods have provided a better understanding of plasma proteins and their roles in different diseases, but are difficult to use for routine disease detection in a clinical setting (Diamandis, 2004) because of the technically demanding and time-consuming sample preparation requirements (Diamandis, 2004; Fujii et al., 2005). 2DGE use is further hindered by its low throughput nature. These limitations are especially true in coagulation diagnostics where point-of-care devices are often needed for emergency or home use. While MS methods are relatively high throughput, they do not necessarily reveal the kinetics or functional interactions within the plasma protease cascades. Currently, activity information is accessed in clinical settings through activated partial thromboplastin time (aPTT) or activated clotting time (ACT, also known as prothrombin time, PT), which crudely measure activity through blood gelation rates. Capturing activity information more efficiently and specifically should provide dramatic increases in diagnostic power.

One way to rapidly and selectively capture protease activity information is to use fluorogenic coumarin substrates (Backes et al., 2000). These substrates become fluorescent upon proteolytic cleavage, thereby allowing for ready detection of protease activity. The challenge is that the proteases in the blood coagulation cascade have overlapping specificities, and no exclusive one-to-one linkage exists between each protease and an individual fluorogenic substrate. As such, we have used solution phase microarrays of a larger set of substrates to profile the individual blood proteases to help define groups of optimal substrate sequences. We then employed various deconvolution algorithms to use these optimal substrates as novel biosensors to investigate the transient state of blood during coagulation. This approach could be clinically useful for detection of enzyme activity directly from plasma samples because it allows direct analysis of small sample quantities.

MATERIALS AND METHODS

Proteases, Plasma, and Fluorogenic Substrates

Purified human plasma kallikrein, human factor Xa, human thrombin and human plasmin were purchased from Enzyme Research Laboratories (South Bend, IN). Human urokinase plasminogen activator (uPA) and lipidated recombinant human tissue factor were purchased from American Diagnostica (Stamford, CT). Whole blood was obtained by venipuncture from healthy, non-smoking volunteers in accordance with protocols approved by the University of Pennsylvania IRB and anticoagulated with 1/9 volume of 3.8% sodium citrate in the syringe (Sigma; St. Louis, MO). Whole blood was centrifuged at 100*g* for 15 min to obtain platelet rich plasma (PRP) followed by centrifugation of the supernatant at 10,000*g* for 5 min to generate platelet free plasma (PFP).

Fluorogenic peptide substrates for plasma kallikrein (Z-FR-MCA, 612.6 MW), factor Xa (Boc-IEGR-MCA, 730.8 MW), thrombin (Boc-VPR-MCA, 627.8 MW), urokinase plasminogen activator (glutaryl-GR-MCA, 502.5 MW) and plasmin (Boc-VLK-MCA, 615.8 MW) were purchased from Bachem (King of Prussia, PA). Three hundred sixty-one fluorogenic substrates were synthesized in a library of the general format Ac-A-P_3-P_2-R-coumarin (where P_3 and P_2 were naturally occurring amino acids except Cys) according to protocols detailed previously (Backes et al., 2000; Gosalia et al., 2005a,b).

Microarray Printing

Lysine coated glass slides (Erie Scientific, New Hampshire) for arraying were cleaned in 100% ethanol and dried. The specific fluorogenic substrates were diluted in 50% glycerol/DMSO to 1 mM prior to arraying and printed in quadruplicates per sub-array with two sub-arrays per slide. The 361 compound fluorogenic substrate library, also in 50% glycerol/DMSO, was printed at 50 μM in a 16×24 format equivalent to a 384-well plate. All slides had internal calibration standards to enable intra- and inter-slide quantification and normalization. The fluorogenic substrates were printed according to protocols previously described (Gosalia et al., 2005a,b). After printing, the slides were refrigerated and stored desiccated and in the dark until use.

Reactions and Data Analysis

The proteases were reconstituted and diluted in buffers recommended by the manufacturers. The proteases and plasma mixtures were individually delivered to the specific

DOI 10.1002/bit

substrate arrays and the 361 compound library as previously described (Gosalia and Diamond, 2003; Gosalia et al., 2005a,b) and underwent ~30-fold dilution from the final delivery concentration after mixing in the microspot (Gosalia and Diamond, 2003; Gosalia et al., 2005a,b).

The final delivery concentrations were: 1 μM plasma kallikrein in 4 mM NaOAc-HCl, 150 mM NaCl (pH 5.3); 20 μM factor Xa in 20 mM Tris, 700 mM NaCl (pH 7.4); 10 μM human thrombin in 50 mM sodium citrate, 200 mM NaCl, 0.1% PEG-8000 (pH 6.5); 10 μM uPA in, 150 mM PBS (pH 7.2); 10 μM plasmin in 100 mM HEPES, 100 mM NaOAc (pH 8.5); 10 μM factor α XIIa in 4 mM NaOAc-HCl, 150 mM NaCl (pH 5.3); 100 nM factor XIa in 4 mM NaOAc-HCl, 150mM NaCl (pH 5.3); 10 μM factor IXa β in 20 mM Tris-HCl, 100 mM NaCl (pH 7.4); 5 μM factor VIIa in 20 mM Tris-HCl, 100 mM NaCl, 1 mM CaCl2 (pH 7.4); and 10 μM APC in 20 mM Tris-HCl, 100 mM NaCl (pH 7.4). Citrated PFP was diluted threefold before being delivered to the specific substrate array and the 361 compound microarray. The mixtures consisted of 1 part citrated plasma, 1 part 30 mM calcium chloride in Hank's balanced salt solution (HBSS) and 1 part activators [kaolin (1.5 mg/mL), tissue factor (81 pM), plasmin (1.5 μM) or uPA (1 μM)]. HBSS buffer was substituted in absence of calcium chloride or activators. Each mixture was incubated for exactly 1 or 10 min at 37°C prior to being used with the enzyme assay microarray, thus representing a transient state of plasma. In the event of a clot formation, the mixture was centrifuged and the serum was used.

The slides ($n = 4$ for specific substrates, $n = 6$ for substrate library) were incubated at 37°C for 30 min to 6 h. This incubation time resulted in ~5 to 25% cleavage of the best substrate on each array, assuring that the assays were run within the linear range. The activated slides were scanned using a cooled CCD-based imager (NovaRay, Alpha Innotech, San Leandro, CA), at Ex λ: 405/40 nm and Em λ: 475/40 nm with integration times of 250 msec and 15 μm pixel resolution. Images were acquired in a 16-bit format and the analysis was performed using Array Vision (Imaging Research, Ontario, Canada).

The percent cleavage for every substrate in the 361 compound library was determined for each protease using the following formula

$$\text{Percent Cleavage}_{i,e} = 1 - \frac{f_{\max,e} - f_{i,e}}{f_{\max,e} - f_{\min,e}} \quad (1)$$

where $f_{\max}$ is the mean fluorescence intensity of the calibration standard ($n = 8$ spots per slide of 50 μM unacylated coumarin), $f_{\min}$ represents mean blank (with no substrate) intensity ($n = 15$ spots/slide) and $f_{i,e}$ stands for the fluorescence of individual substrates (i) after cleavage by a particular enzyme (e). The final cleavage percentages for each substrate in the library were averaged ($n = 6$) and combined to give cleavage percent reference maps for every protease. The maps were represented using Cluster and Treeview (Ewald and Eisenberg, 1995). For the most preferred substrates the signal/background ratio was typically >60 with CV <5%.

Determination of Optimal Substrates

To determine the optimal relative substrate, the cleavage of each substrate (s_i) by a single enzyme (subscript e) was compared to the cleavage of that substrate by all enzymes to determine the specificity (S) in Eqn. 2. At the same time, the cleavage percentage for all substrates was normalized and scaled (C) on the range 0–1 as shown in Eqn. 3. The optimal substrate (Q_e) was determined to be the substrate with a maximum weighted combination of specificity (weighted by w_s) and cleavage percentage (weighted by w_c) as shown in Eqn. 4.

$$S_{i,e} = \frac{s_{i,e}}{\sum_e s_{i,e}} \quad (2)$$

$$C_{i,e} = \frac{s_{i,e} - \min_i(s_{i,e})}{\max_i(s_{i,e}) - \min_i(s_{i,e})} \quad (3)$$

$$Q_e = \max_i(w_s S_{i,e} + w_c C_{i,e}) \quad (4)$$

Several values of w_s and w_c between 0.3 and 0.7 were tested and there was not a significant difference noted in the selected substrates. Also, modifications of Eqn. 4 were tested where the max function was chosen of the product of $S_{i,e}$ and $C_{i,e}$. The product maximization produced poorer results in the diagonalization of the substrate and substrate cocktail matrices. As a result, for all reported results, $w_s = w_c = 0.5$ (Eqn. 4).

Deconvolution of Array Data

The data from the microarrays were deconvoluted using the *lsqnonneg* function from Matlab R14 service pack 2 based on Lawson and Hanson's *nnls* function (Lawson and Hanson, 1974). This function works by computing the value of the regressed weights (W) for a representation of the protease maps as vectors (E) that minimizes the Euclidean distance between the actual plasma maps (A) and the regressed values (R) (Eqns. 5 and 6). The non-negativity constraint was maintained by selecting the most positive element from the regression where all other elements are maintained at 0, holding that element as required, and then repeating the regression with that element non-zero and choosing the next most positive element. It then iterated until the all remaining zero weight elements resulted in negative or zero weights.

$$\min_{W \geq 0} \|A - EW\|_2 \quad (5)$$

$$R_i = \sum_i W_i E_i \quad (6)$$

RESULTS

Fluorogenic Substrate Microarrays for Individual Proteases and Plasma

The fluorogenic peptide substrates Z-FR-MCA, Boc-IEGR-MCA, Boc-VPR-MCA, glutaryl-GR-MCA, and Boc-VLK-

MCA were microarrayed along with fluorescence calibration standards of MCA (7-amino-4-methylcoumarin) and blank spots. These substrates are often matched with individual proteases used for kinetic studies: plasma kallikrein, factor Xa, thrombin, urokinase plasminogen activator, and plasmin, respectively (Morita et al., 1977), although it is well recognized that different blood proteases can cleave each substrate with varying kinetics. The slides were activated individually with purified enzymes or human plasma mixtures and the signal intensities were averaged over $n = 4$ slides (32 spots per substrate) with the internal controls enabling intra- and inter-slide normalization and quantification. A sample set of raw image data is shown Figure 2A for the pure proteases (Fig. 2A, rows 1–5) or plasma samples (Fig. 2A, rows 6–12). The entire data set was averaged (Fig. 2B) to quantify transient activity of the coagulation proteases and then row normalized (Fig. 2C) to help elucidate the specificities of the individual substrates and the different pathways of the coagulation system.

Delivery of human plasma kallikrein to the array (Fig. 2, row 1) resulted in minimal cleavage of the substrates (Fig. 2B) with Z-FR-MCA being the best cleaved substrate (Fig. 2C). In a panel of 20 coumarin substrates, Iwanaga, et al. found substrates with a P_2 Phe residue to be more efficiently cleaved by plasma kallikrein than those with P_2 Gly or Pro (Morita et al., 1977) where $P_1 = \text{Arg}$. The other substrates were also cleaved at lesser but detectable levels as expected (Gosalia et al., 2005b; Morita et al., 1977), as shown in Figure 2C.

Human factor Xa resulted in maximum cleavage of Boc-IEGR-MCA and glutaryl-GR-MCA with detectable cleavage for Z-FR-MCA (Fig. 2, row 2). The physiologic substrates of factor Xa (prothrombin, factor VII and the factor Xa autolysis loop) have a $P_1 = \text{Arg}$, $P_2 = \text{Gly}$ motif (Brandstetter et al., 1996) and several studies using synthetic substrates, including a positional scanning-synthetic combinatorial library (Backes et al., 2000) and a panel of *p*-nitroanilide substrates (Schoen and Lindhout, 1987), have shown a distinct preference for Gly at the P_2 position. However, there exists considerable cooperative interactions between substrate subsites for factor Xa (Gosalia et al., 2005a).

Human thrombin resulted in a specific and intense fluorescence signal from Boc-VPR-MCA that was 65-fold greater than background (Fig. 2, row 3), consistent with the fluorometric properties of the substrate (Morita et al., 1977). In a fluorimetry cuvette, complete conversion of the Boc-VPR-MCA substrate resulted in a 65.2-fold increase in total integrated fluorescence emission over the unconverted substrate (data not shown) when treated with human thrombin.

Similarly, delivery of human uPA to the sensing array caused a specific and intense fluorescence signal from glutaryl-GR-MCA (Fig. 2, row 4), resulting in fluorescence that was ~50-fold above background, consistent with single substrate studies of Morita et al. (1977).

Human plasmin (10 μM) displayed a detectable activity on Z-FR-MCA and Boc-VPR-MCA (Fig. 2A and B, row 5). Morita et al. and Kato et al. had determined that human plasmin cleaved Boc-VLK-MCA, Boc-VPR-MCA and Z-FR-MCA with equivalent efficiency (Morita et al., 1977).

For the purposes of biosensing, an ''ideal'' member of a set of substrates would be cleaved rapidly by only a single protease, thereby producing a fully diagonal 5×5 matrix with no off-diagonal signal for the 5 enzymes tested. Rows

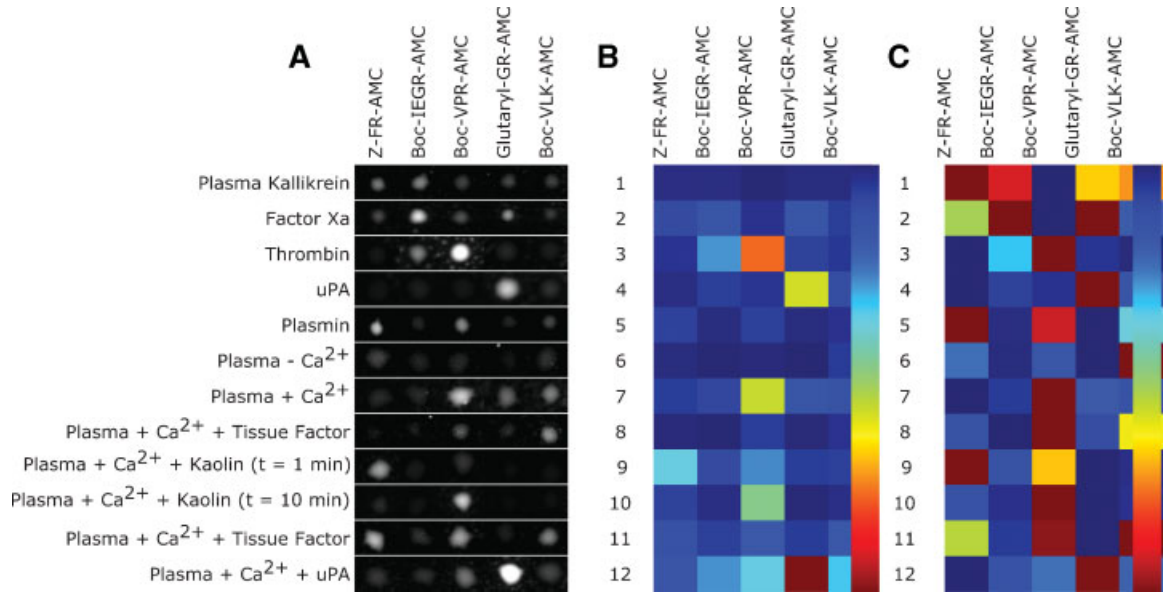

Figure 2. Enzyme assay microarrays. **Panel A** shows the actual arrays treated with the individual enzymes and plasma mixtures. **Panel B** shows the averaged data for each substrate ($n = 32$ spots, linear scale of 0.003 is blue and 0.5 is red) and **Panel C** shows the row normalized data (linear scale of 0–1) to elucidate the specificity of the protease for each substrate. For all figures, low mean fluorescent intensity is blue and it goes through the spectrum to high mean fluorescent intensity being red.

DOI 10.1002/bit

1–5 of Figure 2C show that the set of substrates employed in this experiment displayed a trend toward diagonal dominance but were far from ideal. Only the uPA/glutaryl-GR-MCA and thrombin/Boc-VPR-MCA pairs displayed a fairly high degree of selective signal, although Xa can cleave glutaryl-GR-MCA, thrombin can cleave Boc-IEGR-MCA, and plasmin can cleave Boc-VPR-MCA.

The substrate cleavage signal becomes more complex for protease mixtures found in plasma. Citrated human plasma was diluted (1:3) and recalcified in the presence of different activators (tissue factor, kaolin, plasmin, and uPA) and delivered to the arrays to potentially detect the endogenous levels of plasma kallikrein, factor Xa, thrombin, uPA, and plasmin resulting in ~1:100 final dilution of plasma. The plasma mixtures were incubated with the activators for different lengths of time ($t = 1$ or 10 min) before delivery to the arrays. Almost no substrate cleavage was observed when the array was treated with citrated plasma (Fig. 2, row 6). Recalcified citrated plasma (10 min) resulted in elevated cleavage of all five substrates (row 7) relative to citrated plasma (row 6). Recalcification of citrated plasma in the presence of lipidated tissue factor (27 pM) for 10 min before delivery to the microarray (row 8) resulted in Boc-VPR-MCA cleavage. Cleavage of this substrate is likely to be due to the product of tissue-factor initiated cascade (Fig. 1), thrombin, which readily cleaves Boc-VPR-MCA (row 3).

Rows 9 and 10 (Fig. 2) show the profile of recalcified citrated plasma when activated with kaolin, a contact pathway activator (Griffin and Cochrane, 1976) at different incubation times of 1 or 10 min. The profiles (Fig. 2, rows 9 and 10) show us the transient progress of the contact activated system on the array with different substrates being cleaved at the two time points, resulting in significant cleavage of Z-FR-MCA after 1 min and Boc-VPR-MCA after 10 min. This result is consistent with kaolin initially activating plasma kallikrein (resulting in cleavage of Z-FR-MCA), which initiates the intrinsic cascade (Fig. 1) to produce active thrombin (resulting in cleavage of Boc-VPR-MCA). The generation of thrombin is confirmed by the observance of clotting after the 10 min incubation. At the 10 min time point, we observed reduced activity of the plasma kallikrein substrate in serum, as would be expected if the kallikrein in the mixture has been inhibited by kallistatin or a kallistatin precursor (Chao et al., 2001) after its activation of the coagulation cascade.

Addition of plasmin to recalcified citrated plasma (incubation time = 10 min) led to significant cleavage of each substrate on the array (Fig. 2, row 11). Strong signals in the plasma kallikrein, thrombin and plasmin substrate spots, with reduced signals in the factor Xa and uPA substrates were observed (Fig. 2, row 11). A higher level of kallikrein substrate Z-FR-MCA conversion was noted in the plasmin treated-plasma (Fig. 2A and B, row 11) beyond that expected from plasmin-mediated conversion of the substrate, indicating that plasmin-activated thrombin (Ewald and Eisenberg, 1995) may have converted prekallikrein to kallikrein (Hoffmeister et al., 2001).

Similar to addition of a high concentration of plasmin, addition of uPA to recalcified citrated plasma caused high levels of cleavage of all five substrates (Fig. 2, row 12). Endogenously, urokinase is present at very low concentrations, nearly 100,000-fold lower than plasminogen (Rijken and Sakharov, 2001). Thus, addition of a high dose of uPA may have resulted in activation of plasminogen and plasmin-mediated generation of XIIa (Ewald and Eisenberg, 1995) with consequent kallikrein generation to an extent comparable to adding high levels of plasmin to the plasma. This pathway has been documented during thrombolytic therapy (Ewald and Eisenberg, 1995; Mayer, 1990). Activation of XIIa and kallikrein results in initiation of the coagulation cascade resulting in cleavage of the factor Xa and thrombin substrates (Fig. 1).

Purified Proteases and Plasma Activation of the 361-Compound Fluorogenic Library

Given some of the limitations observed with commercially available substrates with respect to forming a fully diagonalized 5×5 matrix for the limited set of enzymes tested, we next explored whether a larger array of compounds could provide a more ideal set of substrates. A total of 10 purified human plasma proteases as well as various human plasma preparations were tested against a 361-compound library (Fig. 3). The specificities and optimal fluorogenic substrates for the five human proteases of plasma kallikrein, factor Xa, thrombin, uPA, and plasmin, listed in Table I, are in accordance with literature (Gosalia et al., 2005a,b).

With the large database of experimental data shown in Figure 3, three separate protocols were employed to help analyze the data and to help develop strategies for deconvolution of protease activity signals from within a protease mixture as complicated as human plasma. The first protocol (Fig. 4) searched for a single ''optimal'' sensing substrate sequences for the 5 enzymes used in Figure 2, in order to compare this approach with results found with commercial substrates and to understand if improvement over the commercial substrates was possible. The second protocol (Fig. 5) ranked nine ''optimal'' sensing substrates via Eqn. 4 for all 10 purified enzymes tested in Figure 3 and found the top 9 substrates for each enzyme (Fig. 5A). Then, each group of optimal 9 substrates for each of the 10 enzymes was bundled via weighted averaging into a super-pixel that had biosensing properties not obtainable by any individual fluorogenic substrate (Fig. 5B) in order to produce a highly diagonal-dominant 10×10 row-normalized matrix (Fig. 5C). The third protocol (Fig. 6) treated each 361-element map measured for each plasma preparation as a weighted sum of the 10 maps obtained for the 10 purified enzymes. The third protocol represents a deconvolution strategy via global minimization of error whereas the second protocol represents a deconvolution strategy via 10 local minimizations of error around the 10 purified enzymes. In the presentation of these three protocols, the term ''biosensor'' is used with respect to the response of the defined set of

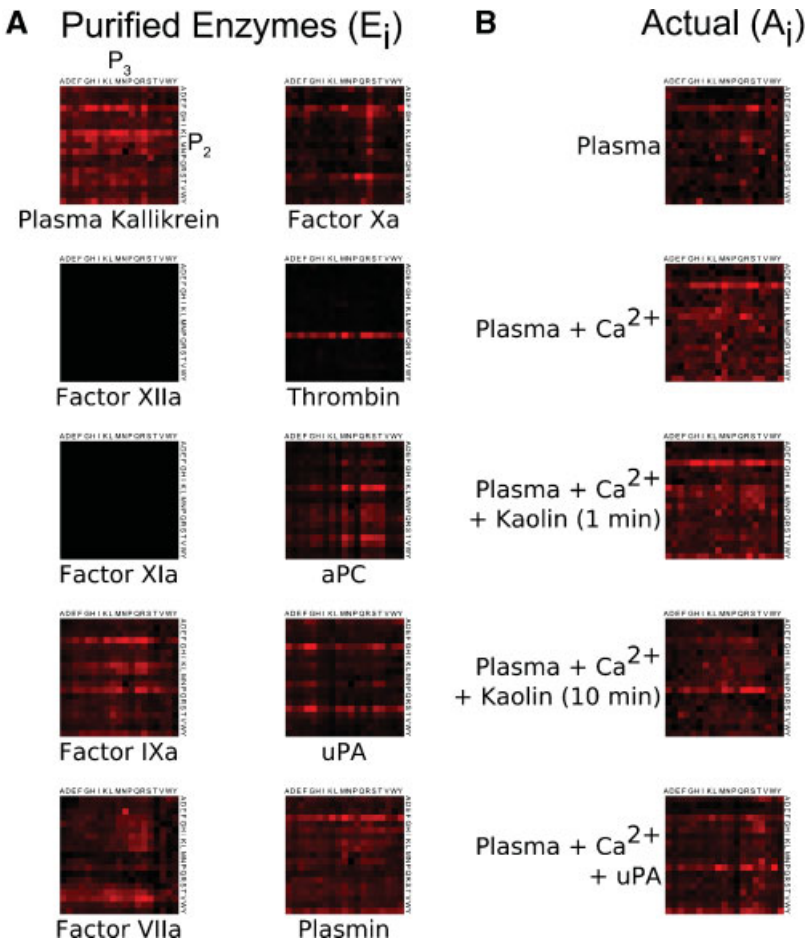

Figure 3. Substrate specificities of human serine plasma proteases. **Panel A** characterizes the specificity of plasma serine proteases using the Ac-Ala-P_3-P_2-Arg-ACC-NH_2 substrate microarrays. **Panel B** characterizes plasma with the same substrate microarray. Each square in the grid is colored in proportion to the average ($n = 6$) quantitated fluorescence intensity of the corresponding substrates, after treatment with the enzyme, indicating the relative amount of cleavage. The vertical axis indicates the P_2 residue and the horizontal axis indicates the P_3 residues in order of A, D, E, F, G, H, I, K, L, M, N, P, Q, R, S, T, V, W, and Y.

substrates under consideration. The term ''enzyme signal'' (for example, the ''thrombin signal'') denotes an observed response of the biosensor which, while likely indicative of a specific enzyme activity (e.g., thrombin), is not direct proof of the enzyme activity (as would be the detection of thrombin-antithrombin complex, thrombin activation peptide, or fibrin).

Table I. Optimal Substrates for Kallikrein, Factor Xa, Thrombin, uPA, and Plasmin.

Enzyme	P_1	P_2	P_3	Optimal substrate
Kallikrein	R	K > F, L > N > T, Y	R > H > A, E, L, G	Ac-AMLR-ACC
Factor Xa	R	F > S > G	R	Ac-ARSR-ACC
Thrombin	R	P	Broad	Ac-AMPR-ACC
uPA	R	G > S > A, H, N > T	G > S > T	Ac-AGGR-ACC
Plasmin	R	F > Y > H	M > Q, R	Ac-AMFR-ACC

The substrates given for P_2 and P_3 are the results that would be obtained from a split-pool method. While the optimal substrate determined from each compound individually. Also, the optimal substrate may not be the same as indicated by split pool methods because of another enzyme cleaving those indicated by the split pool methods.

Protocol 1: Optimal Substrates for Plasma Kallikrein, Xa, Thrombin, uPA, and Plasma

Optimal substrate sequences were selected from the library for each of the five human plasma proteases previously studied in Figure 2 using the individual protease maps and Eqn. 4. An ''optimal'' substrate is defined by Eqn. 4 and does not necessarily specify the substrate that is cleaved fastest by a particular enzyme. Many substrates that are rapidly cleaved are non-specific, and hence may be dependent on multiple enzymes in the milieu. Other substrates, while poorly cleaved, may be very specific and thus linearly independent in a mathematical sense. The term optimal substrate indicated the highest ranked substrate from a predetermined set of substrates (361 compounds in our case) that provided the best combination of specificity and cleavage within this set of enzymes as determined by Eqn. 4.

Using the maps shown in Figure 3, the percent cleavage of each highest ranked optimal substrate for kallikrein (AMLR), factor Xa (ARSR), thrombin (AMPR), uPA (AGGR), and plasmin (AMFR) is shown in Figure 4A (rows 1–5). When comparing the row normalized signal for rows

DOI 10.1002/bit

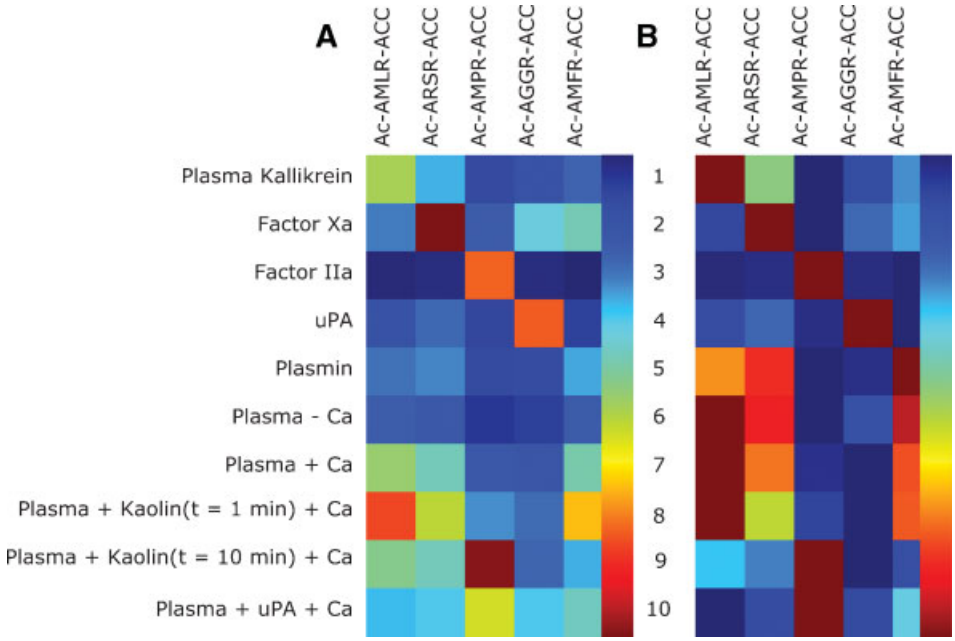

Figure 4. Selection of optimal substrates. **A**: Shows the optimal substrates chosen from Figure 2 and averaged ($n = 6$, linear scale of 0.006–0.53) and (**B**) shows the row normalized data (linear scale of 0–1). These substrates were chosen by the criteria of Eqn. 4 where $w_c = w_s = 0.5$. Note that these substrates may not be the best substrate when chosen with a larger set of proteases.

1–5 of Figure 2B with Figure 4B, the selected optimal substrates (Table I) significantly improved the quality of the biosensing single (diagonal-dominance) compared to the commercially available substrates.

The optimal substrates showed minimal cleavage activity, comparable to background levels, for citrated plasma (Fig. 4A, row 6) with a trace of kallikrein and plasmin signals detected by the row-normalized biosensor (Fig. 4B, row 6), consistent with the results obtained in Figure 2B and C, row 6. Recalcification of citrated plasma for 10 min enhanced the kallikrein and plasmin signal detected by the biosensor with very slight detection in the levels of the factor Xa and uPA signal detected by the biosensor. While plasma kallikrein can cleave the optimal plasmin substrate (Ac-AMFR-coumarin), it does so with less efficiency than its own substrate (Ac-AMLR-coumarin). The high signals for both the plasmin and kallikrein signals observed in the biosensor suggest that both plasma kallikrein and plasmin were present

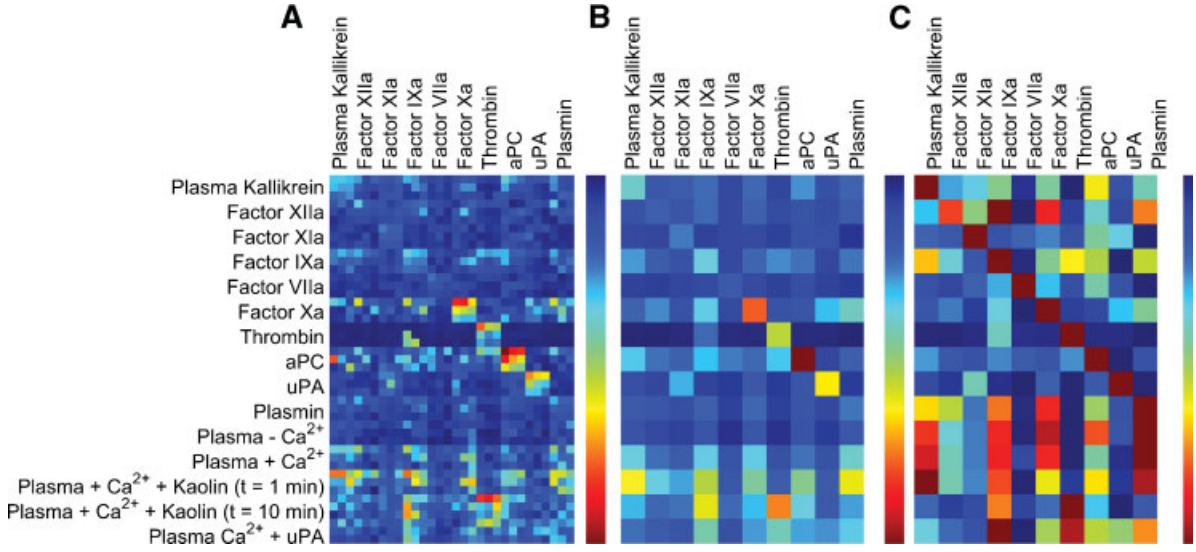

Figure 5. Determination of optimal substrate cocktails. The optimal substrate cocktails were chosen by application of Eqn. 4 where $w_c = w_s = 0.5$. **Panel A** shows 3×3 arrays of substrates for each protease. The substrates chosen are listed in Table II. **Panel B** is a weighted average of the substrate cocktails that would be similar to the result given by a mixture of the substrates in a single well (weight factors are also given in Table II). **Panel C** is a row normalized version of **panel B**; it demonstrates the strong specificity that can be seen of each substrate cocktail for its protease. The only substrate that is not preferential for its cocktail is XIIa, which shows very low cleavage of any of the available substrates.

in the recalcified citrated plasma. There was no detectable activity of thrombin signal detected on the biosensor for recalcified plasma (10 min) as compared to Figure 2B and C, where thrombin showed maximal signal for Boc-VPR-MCA. The absence of thrombin in recalcified citrated plasma can also be seen from the recalcified citrated plasma map (Fig. 3), which showed no P_2 = proline band. Thus, the detection of a thrombin signal in Figure 2 using Boc-VPR-MCA from recalcified citrated plasma mixture was below detection with the optimal substrates.

Cleavage of the optimal substrates on the biosensor for mixtures of recalcified citrated plasma and kaolin (500 μg/ml, final concentration) are shown in Figure 4, rows 8 and 9. Again, plasmin and plasma kallikrein signals with slight detectable levels of factor Xa and uPA signals observed with the biosensor for the 1 min incubation of recalcified plasma with kaolin (Fig. 4, row 8). This result was no different from row 7 except for higher transient levels were observed for both the plasma kallikrein and plasmin signals, as determined by their cleavage activity. This was expected because kaolin is an activator of the contact pathway (Griffin and Cochrane, 1976). Clotting was observed in the vial containing the 10 min pre-incubated mixture of plasma and kaolin (proof of thrombin activity); therefore, the serum supernatant of the clot was delivered to the 361 compound library. In this case, thrombin, plasma kallikrein, plasmin, and factor Xa signals were detected with the biosensor.

Addition of uPA to plasma (Fig. 4, row 10) will activate plasminogen to plasmin, which in turn can mediate the activation of factor XII and subsequent downstream thrombin generation (Ewald and Eisenberg, 1995). Cleavage of Ac-AMFR-coumarin, the optimal substrate for plasmin, in row 10 (Fig. 4A) is not likely due to the presence of transient levels of plasma kallikrein or factor Xa in the plasma and uPA mixture, but due to the presence of transient levels of plasmin generated by the uPA. This conclusion is suggested because there is minimal cleavage of the optimal substrates for plasma kallikrein and factor Xa. In contrast, using the commercial substrates (Fig. 2), factor Xa and plasma kallikrein signals were observed upon addition of uPA to plasma. This could be attributed to the non-specificity and cross reactivity of the substrates (kallikrein substrate Z-FR-MCA can be cleaved by plasmin and factor Xa substrate Boc-IEGR-MCA can be cleaved by uPA and thrombin), indicating that the larger library of substrates allows for more selective detection.

Protocol 2: Optimal Substrates for Kallikrein, and Factors XIIa, XIa, IXa, VIIa, Xa, Thrombin, aPC, uPA, Plasmin

Using the full cleavage maps for 10 individual proteases in Figure 3, we ranked the top 9 optimal substrates for each protease (Fig. 5A, rows 1–10). We then performed a weighted average of the substrates using the quality scores as weights (from Eqn. 4) to create a bundled signal presented as a super-pixel in Figure 5B. This averaged signal is equivalent to that which would be observed if fluorescence were measured from a tube containing that cocktail of substrates. This approach produced a diagonal-dominant 10×10 biosensor (Fig. 5C, rows 1–10). Using Eqn. 4, we determined a substrate cocktail that was specific for most of the tested proteases; the only protease for which the substrate biosensing cocktail was not highly specific (not diagonally dominant) was factor XIIa, which preferentially cross-talked with the factor IXa cocktail. Kallikrein and factor IXa were diagonally-dominant, but had some off-diagonal cross-talk with the aPC biosensing cocktail and the factor IXa and thrombin biosensor cocktails, respectively.

Using the data sets from Figure 3 for human plasma subjected to various treatments and the optimal substrates selected and processes as described above, the enzyme signals in human plasma were analyzed. As expected, citrated plasma without calcium showed little activity across all the substrate cocktails used to detect the 10-protease signals (Fig. 5B, row 11). When row-normalized, trace signals for plasmin, factors Xa and IXa, and kallikrein were detectable in citrated plasma. Plasma with calcium (10 min) showed more signals than citrated plasmin with stronger signals detected for kallikrein, factor Xa, factor IXa, and plasmin although factor IXa and plasmin may be showing up as cross reactivity with factor Xa), suggesting early phase initiation of coagulation prior to the explosive burst in thrombin production.

At 1 min, kaolin maximally activated the contact coagulation pathway with signals apparent for kallikrein, plasmin, aPC, and factors XIIa, IXa, Xa. After 10 min of kaolin treatment, a clot formed and a significant amount of thrombin signal was detected in the serum. Finally, when plasma was activated with uPA and Ca^{2+}, factor XIIa and plasmin signals were detected, indicating the initiation the coagulation cascade. Importantly as is shown by the increased number of enzymes in Figure 3 when compared to Figure 2, this protocol allows for detection of many more enzymes simultaneously than the commercially available probes or protocol 1.

Protocol 3: The 361-Element Plasma Biosensor as Weighted Sum of Total Protease Maps

In an attempt to use all data available for the deconvolution and detection of proteases present within plasma, we used Lawson and Hanson's method of non-negative least square fitting to deconvolute the data (Lawson and Hanson, 1974). The actual, experimentally-determined plasma maps (Fig. 3B) were used to generate regressed maps (Fig. 6A) based on the weighted sum (Fig. 6B) of the individual protease maps (Fig. 3A). Ideally, the deconvolution would give weights W_i (Fig. 6B) that can be related to the time integral of the instantaneous concentrations of the proteases in plasma. In comparing the weights W_i in Figure 6C with the bundled pixels of Figure 5B, a similar set of signals emerge for the treated plasmas. As expected, endogenous factor VIIa signal was below detection since exogenous tissue

DOI 10.1002/bit

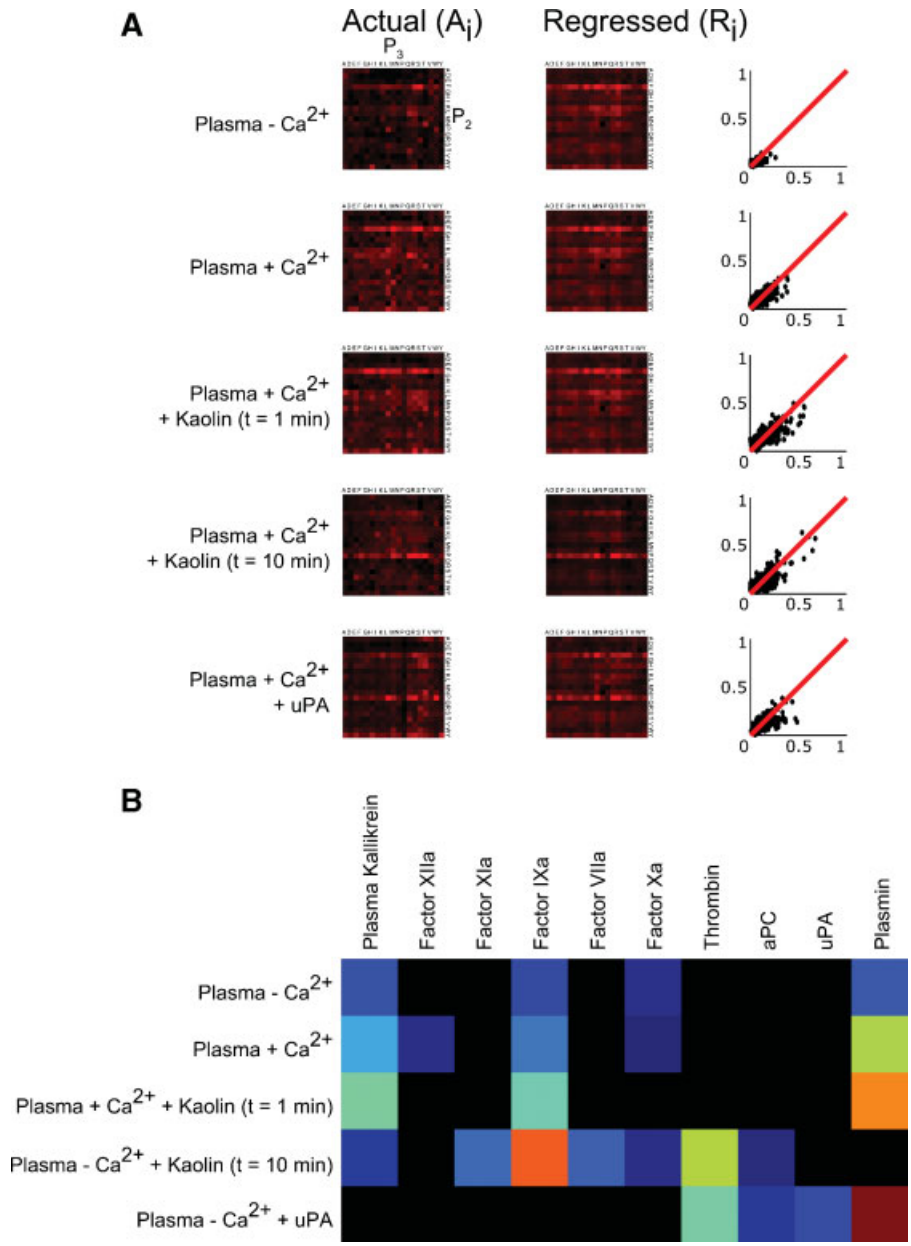

Figure 6. Deconvolution of 361-substrate biosensor signal for plasma based on purified protease maps. In **panel A**, the first column is the actual data from plasma maps while the second column represents the regression of the values by application of Eqns. 5 and 6 to the 10 individual proteases and the five plasma conditions. The third column illustrates the fit where the x-axis is the actual data, the y-axis is the regressed data, and the red line is the y = x line where perfect fit would be indicated. **Panel B** is a representation of the weights where the deconvoluted active proteases are visible as the non-black data with blue as low values and red as high, and the proteases with no activity according to the deconvolution are shown as black.

factor was not added. This is expected since both are derived from the same data in Figure 3 and indicates that a small subset of fewer than 90 substrates (9 substrates $\times$10 enzymes) within the 361-set of sequences contains the majority of biochemical information, the remainder of substrates are redundant, too non-specific, or produce too little signal to contribute to deconvolution. Clinically, the methods may be improved upon by further minimization of the number of substrates or including specific inhibitors in the microarray spots to help distinguish the activity of particular enzymes.

CONCLUSION

We have tested enzyme assay microarrays to evaluate protease specificities and activities against different substrates using purified enzymes and human plasma activated by various treatments. The separation-free assay of numerous enzymatic activities under a wide variety of reaction conditions using a small biological sample ($<$5 µl per slide) represents a common challenge in proteomics. This method offers the versatility of solution phase reaction assembly where substrates, cofactors, or inhibitors can be controlled at

each position on the array using standard microarraying techniques (Gosalia and Diamond, 2003).

Overlapping substrate specificities of many plasma proteases (Gosalia et al., 2005a,b) makes it very difficult to accurately detect the presence of transient levels of a specific protease from a complex milieu of proteases, posing a challenge for clinical diagnostics. We tested currently available substrates for five coagulation proteases—plasma kallikrein, factor Xa, thrombin, uPA, and plasmin. The substrates were highly non-specific, making it difficult to accurately detect the presence of a protease from a complex mixture like plasma (Fig. 2).

Our microarray-based method enabled us to determine optimal substrates for the five coagulation proteases tested from a 361 compound fluorogenic library. These substrates overcame the cross-reactivity and non-specificity of currently available ''specific'' substrates (Fig. 4, rows 1–5) by accurately determining the presence of different proteases from a complex mixture like plasma and can be potentially used for diagnosing various coagulopathies or functional phenotyping. The surprisingly strong signal from factor IXa in Figure 5 indicates that we may have found a method of detecting factor IXa directly within complex fluid mixtures instead of indirect methods of detection currently used (Butenas et al., 2004).

The utility of the biosensor is underscored by studying the apparent proteolytic activities in the kaolin-activated plasma. While the commercial substrates indicated only kallikrein activity after 1 min (Fig. 2), with the cocktail of substrates (Fig. 5, Table II), we were able to detect the relative activities of many enzymes simultaneously, observing activity of kallikrein, factors XIIa, IXa, and Xa, as well as aPC, and plasmin. These protease activities are not unexpected: contact activation of the coagulation cascade is expected to increase factor XIIa concentration, which would increase plasma kallikrein activity (Cochrane and Griffin, 1982; Griffin and Cochrane, 1976). Factor XIIa would also be expected to result in activation of factor IXa, which would subsequently activate factor Xa, leading to thrombin generation (Davie and Ratnoff, 1964). More factor IXa is present due to thrombin feedback to factor XIa (Gailani and Broze, 1991). The observed plasmin signal could be due to either kallikrein-induced activation of prourokinase and, subsequently, plasminogen (Yamamoto et al., 1983) or the thrombin generation cascade may have activated the fibrinolytic pathway with subsequent activation of plasmin and uPA (Butenas et al., 2004).

After 10 min incubation with kaolin, the biosensor only reported activity of thrombin and factor IXa. The diminished signal of factor XIIa after the 10 min incubation can be attributed to C1 inhibitor inhibition of factor XIIa (Bos et al., 2003; Wuillemin et al., 1996). Reduced Xa activity can be attributed to the presence of tissue factor pathway inhibitor (TFPI) and antithrombin-III (ATIII) (Hockin et al., 2002; Mann et al., 2003; van 't Veer and Mann, 1997), which are generated after thrombin production surpasses the threshold limit thereby reducing the activity of coagulation cascade. Reduced activity for uPA and plasmin is observed due to reduced activity of kallikrein or depletion due to their fibrinolytic activities.

We have also shown a proof of concept of rapidly deconvoluting the protease proteome in plasma with our 361-substrate library. This work may allow rapid, quantitative analysis of blood pathophysiology using a minimal volume of plasma. It also may allow determination of a protease concentration in plasma without the requirement of determining specific marker substrates. Other deconvolution methods beyond the Lawson–Hanson non-negative least squares could be attempted including determining the minimum angle between the multi-dimensional map vectors of the milieu and the map vectors of the individual proteases. This could be augmented by a test where the angle between the milieu map vector and an orthogonalized null space (or kernel) of the individual protease map vectors would be an indicator of how significant an amount of protease activity and specificity was not accounted for by the tested proteases. A testing limitation to be aware of for all these methodologies is that one cannot test for more proteases than substrates by any method because of linear dependences. In our tests, we examine a maximum of 10 proteases against a 361 compound library and therefore have $<3\%$ of the system dimensionality mapped by our proteases. An additional test that could be

Table II. Optimal Substrate Sequences (Rank Ordered).

	Kallikrein	XIIa	XIa	IXa	VIIa	Xa	Thrombin	aPC	uPA	Plasmin
1	AGFR	AMFR	AFNR	ARFR	ARVR	APSR	AMPR	AMLR	AFGR	AMFR
2	ALFR	AQFR	AFAR	ANFR	AKVR	ARSR	ARPR	ATLR	AGGR	ATFR
3	AKLR	ALFR	AENR	AQFR	AQVR	AYFR	AQPR	ASLR	AGSR	ASFR
4	AMLR	ANFR	AFTR	AQPR	ASVR	ARGR	ALPR	AQLR	AFSR	ALFR
5	AHLR	AMTR	AFSR	ALFR	ANER	AMFR	AYPR	AQTR	ASGR	AYFR
6	AHFR	AYFR	ANTR	AMFR	APVR	ARFR	ATPR	AMTR	ATGR	AQFR
7	AAKR	ANTR	ASNR	ARPR	AMVR	AQSR	AEPR	ARTR	AAGR	AYYR
8	AGKR	AMSR	AGNR	AMPR	AAVR	ARHR	AVPR	ASTR	ASSR	ARFR
9	ARLR	AMDR	AKTR	APFR	ALVR	ASFR	ASPR	ATTR	AWGR	AHFR

This is the list of substrates that were used for the cocktails of 9 substrates (all substrates should be prepended with Ac—and appended with—coumarin). Note that these substrates may be different than the best substrate determined in the 5 enzyme system because more enzymes are taken into account and these additional enzymes might lower the specificity portion of the optimal score.

DOI 10.1002/bit

performed using either of the above methods is to utilize the kinetics of the proteolysis of the substrate by the protease. The kinetic measurements of the activity of each protease against the library could be compared to the activity against a milieu.

Our microarray-based method can also enhance biomarker discovery. We can rapidly profile transient state kinetics of complex biological fluids (such as cell lysate, tissue lysate, conditioned medium, or biological fluid such as blood, urine, or saliva), against an entire positional scanning fluorogenic library with nearly all different amino acids in the P_1 through P_4 positions. Thus the enzyme assay microarrays could facilitate evaluation of metalloproteinases and their inhibitors during matrix remodeling or metastasis, caspase cascades in apoptosis; kinase/phosphatase regulation in intracellular signal transduction and cell cycle regulation, drug screening for inhibitor or regulatory activities against a spectrum of proteases targets, or phenotyping of patients for optimal drug treatment regimes.

ABBREVIATIONS

2DGE	2-dimensional gel electrophoresis
ACT	activated clotting time
aPC	activated protein C
aPTT	activated partial thromboplastin time
ATIII	antithrombin-III
HBSS	Hank's balanced salt solution
IIa	thrombin
MCA	7-amino-4-methylcoumarin
MS	Mass spectrometric
PFP	platelet free plasma
PRP	platelet rich plasma
PT	prothrombin time
TF	tissue factor
TFPI	tissue factor pathway inhibitor
uPA	urokinase plasminogen activator

References

Anderson NL, Anderson NG. 2002. The human plasma proteome: History, character, and diagnostic prospects. Mol Cell Proteomics 1(11):845–867.

Anderson NL, Polanski M, Pieper R, Gatlin T, Tirumalai RS, Conrads TP, Veenstra TD, Adkins JN, Pounds JG, Fagan R, Lobley A. 2004. The human plasma proteome: A nonredundant list developed by combination of four separate sources. Mol Cell Proteomics 3(4):311–326.

Backes BJ, Harris JL, Leonetti F, Craik CS, Ellman JA. 2000. Synthesis of positional-scanning libraries of fluorogenic peptide substrates to define the extended substrate specificity of plasmin and thrombin. Nat Biotechnol 18(2):187–193.

Bertina RM, Koeleman BP, Koster T, Rosendaal FR, Dirven RJ, de Ronde H, van der Velden PA, Reitsma PH. 1994. Mutation in blood coagulation factor V associated with resistance to activated protein C. Nature 369(6475):64–67.

Bogdanov VY, Balasubramanian V, Hathcock J, Vele O, Lieb M, Nemerson Y. 2003. Alternatively spliced human tissue factor: A circulating, soluble, thrombogenic protein. Nat Med 9(4):458–462.

Bos IG, Lubbers YT, Roem D, Abrahams JP, Hack CE, Eldering E. 2003. The functional integrity of the serpin domain of C1-inhibitor depends on the unique N-terminal domain, as revealed by a pathological mutant. J Biol Chem 278(32):29463–29470.

Brandstetter H, Kuhne A, Bode W, Huber R, von der Saal W, Wirthensohn K, Engh RA. 1996. X-ray structure of active site-inhibited clotting factor Xa. Implications for drug design and substrate recognition. J Biol Chem 271(47):29988–29992.

Burke W. 2003. Genomics as a probe for disease biology. N Engl J Med 349(10):969–974.

Butenas S, Orfeo T, Gissel MT, Brummel KE, Mann KG. 2004. The significance of circulating factor IXa in blood. J Biol Chem 279(22): 22875–22882.

Butenas S, Bouchard BA, Brummel-Ziedins KE, Parhami-Seren B, Mann KG. 2005. Tissue factor activity in whole blood. Blood 105(7):2764–2770.

Chao J, Miao RQ, Chen V, Chen LM, Chao L. 2001. Novel roles of kallistatin, a specific tissue kallikrein inhibitor, in vascular remodeling. Biol Chem 382(1):15–21.

Cochrane CG, Griffin JH. 1982. The biochemistry and pathophysiology of the contact system of plasma. Adv Immunol 33:241–306.

Davie EW, Ratnoff OD. 1964. Waterfall sequence for intrinsic blood clotting. Science 145:1310–1312.

Diamandis EP. 2004. Mass spectrometry as a diagnostic and a cancer biomarker discovery tool: Opportunities and potential limitations. Mol Cell Proteomics 3(4):367–378.

Ewald GA, Eisenberg PR. 1995. Plasmin-mediated activation of contact system in response to pharmacological thrombolysis. Circulation 91(1):28–36.

Fujii K, Nakano T, Kanazawa M, Akimoto S, Hirano T, Kato H, Nishimura T. 2005. Clinical-scale high-throughput human plasma proteome analysis: Lung adenocarcinoma. Proteomics 5(4):1150–1159.

Gailani D, Broze GJ, Jr. 1991. Factor XI activation in a revised model of blood coagulation. Science 253(5022):909–912.

Gosalia DN, Diamond SL. 2003. Printing chemical libraries on microarrays for fluid phase nanoliter reactions. Proc Natl Acad Sci USA 100(15): 8721–8726.

Gosalia DN, Salisbury CM, Ellman JA, Diamond SL. 2005a. High throughput substrate specificity profiling of serine and cysteine proteases using solution-phase fluorogenic peptide microarrays. Mol Cell Proteomics 4(5):626–636.

Gosalia DN, Salisbury CM, Maly DJ, Ellman JA, Diamond SL. 2005b. Profiling serine protease substrate specificity with solution phase fluorogenic peptide microarrays. Proteomics 5(5):1292–1298.

Griffin JH, Cochrane CG. 1976. Mechanisms for the involvement of high molecular weight kininogen in surface-dependent reactions of Hageman factor. Proc Natl Acad Sci USA 73(8):2554–2558.

Hockin MF, Jones KC, Everse SJ, Mann KG. 2002. A model for the stoichiometric regulation of blood coagulation. J Biol Chem 277(21): 18322–18333.

Hoffmeister HM, Szabo S, Helber U, Seipel L. 2001. The thrombolytic paradox. Thromb Res 103(Suppl 1):S51–S55.

Lawson C, Hanson R. 1974. Solving least squares problems. Englewood Cliffs, NJ: Prentice Hall.

Liotta LA, Ferrari M, Petricoin E. 2003. Clinical proteomics: Written in blood. Nature 425(6961):905.

Lo K, Diamond SL. 2004. Blood coagulation kinetics: High throughput method for real-time reaction monitoring. Thromb Haemost 92(4):874–882.

Mann KG, Butenas S, Brummel K. 2003. The dynamics of thrombin formation. Arterioscler Thromb Vasc Biol 23(1):17–25.

Mayer M. 1990. Biochemical and biological aspects of the plasminogen activation system. Clin Biochem 23(3):197–211.

Morita T, Kato H, Iwanaga S, Takada K, Kimura T. 1977. New fluorogenic substrates for alpha-thrombin, factor Xa, kallikreins, and urokinase. J Biochem (Tokyo) 82(5):1495–1498.

Petricoin EF, Rajapaske V, Herman EH, Arekani AM, Ross S, Johann D, Knapton A, Zhang J, Hitt BA, Conrads TP, Veenstra TD, Liotta LA, Sistare FD. 2004. Toxicoproteomics: Serum proteomic pattern diagnostics for early detection of drug induced cardiac toxicities and cardioprotection. Toxicol Pathol 32 (Suppl 1):122–130.

Rijken DC, Sakharov DV. 2001. Basic principles in thrombolysis: Regulatory role of plasminogen. Thromb Res 103(Suppl 1):S41–S49.

Schneppenheim R, Budde U, Obser T, Brassard J, Mainusch K, Ruggeri ZM, Schneppenheim S, Schwaab R, Oldenburg J. 2001. Expression and characterization of von Willebrand factor dimerization defects in different types of von Willebrand disease. Blood 97(7):2059–2066.

Schoen P, Lindhout T. 1987. The in situ inhibition of prothrombinase-formed human alpha-thrombin and meizothrombin(des F1) by antithrombin III and heparin. J Biol Chem 262(23):11268–11274.

van 't Veer C, Mann KG. 1997. Regulation of tissue factor initiated thrombin generation by the stoichiometric inhibitors tissue factor pathway inhibitor, antithrombin-III, and heparin cofactor-II. J Biol Chem 272(7):4367–4377.

Wuillemin WA, Eldering E, Citarella F, de Ruig CP, ten Cate H, Hack CE. 1996. Modulation of contact system proteases by glycosaminoglycans. Selective enhancement of the inhibition of factor XIa. J Biol Chem 271(22):12913–12918.

Yamamoto J, Okamoto U, Morita S, Kikui K, Fujii Y. 1983. Production of the modified form of human plasminogen in the plasma activated by urokinase. Jpn J Physiol 33(3):469–484.

DOI 10.1002/bit